Ninein is released from the centrosome and moves bi-directionally along microtubules

David K. Moss[1,*], Gemma Bellett[1], Jane M. Carter[1], Mirjana Liovic[2,3], Jennifer Keynton[1], Alan R. Prescott[4], E. Birgitte Lane[2] and Mette M. Mogensen[1,‡]

[1]School of Biological Sciences, University of East Anglia, Norwich, NR4 7TJ, UK
[2]Division of Cell and Developmental Biology, College of Life Sciences, University of Dundee, Dundee, DD1 5EH, UK
[3]Medical Centre for Molecular Biology, Faculty of Medicine University of Ljubljana, Vrazov trg 2, SI-1000 Ljubljana, Slovenia
[4]Division of Cell Biology and Immunology, College of Life Sciences, University of Dundee, Dundee, DD1 5EH, UK
*Present address: School of Medical Sciences, University Walk, Bristol, BS8 1TD, UK
‡Author for correspondence (e-mail: m.mogensen@uea.ac.uk)

Accepted 26 June 2007
Journal of Cell Science 120, 3064-3074 Published by The Company of Biologists 2007
doi:10.1242/jcs.010322

Summary

Cell-to-cell contact and polarisation of epithelial cells involve a major reorganisation of the microtubules and centrosomal components. The radial microtubule organisation is lost and an apico-basal array develops that is no longer anchored at the centrosome. This involves not only the relocation of microtubules but also of centrosomal anchoring proteins to apical non-centrosomal sites. The relocation of microtubule minus-end-anchoring proteins such as ninein to the apical sites is likely to be essential for the assembly and stabilisation of the apico-basal arrays in polarised epithelial cells. In this study, we establish that ninein is highly dynamic and that, in epithelial cells, it is present not only at the centrosome but also in the cytoplasm as distinct speckles. Live-cell imaging reveals that GFP-ninein speckles are released from the centrosome and move in a microtubule-dependent manner within the cytoplasm and thus establishes that epithelial cells possess the mechanical means for relocation of ninein to non-centrosomal anchoring sites. We also provide evidence for the deployment of ninein speckles to apical anchoring sites during epithelial differentiation in both an in situ tissue and an in vitro culture system. In addition, the findings suggest that the non-centrosomal microtubule anchoring sites associate with adherens junctions in polarised epithelial cells.

Supplementary material available online at
http://jcs.biologists.org/cgi/content/full/120/17/3064/DC1

Key words: Centrosome, Ninein, Polarised epithelial cells, Cochlea, Apico-basal microtubule arrays

Introduction

Differentiation and polarisation of epithelial cells involve a dramatic reorganisation of the microtubule cytoskeleton and centrosomal components. The centrioles migrate to the apical cell surface, the radial microtubule array is largely lost and an apico-basal array develops that is no longer anchored at the centrosome (Bacallao et al., 1989; Bre et al., 1987; Bre et al., 1990; Meads and Schroer, 1995; Tucker et al., 1992). We have previously proposed that a release-and-capture mechanism is responsible for the generation of non-centrosomal apico-basal arrays in most centrosome-containing polarised epithelial cells. This not only involves centrosomal nucleation, release and repositioning of microtubules but also the relocation of centrosomal anchoring proteins such as ninein to apical non-centrosomal anchoring sites (Mogensen, 2004; Mogensen, 1999; Mogensen et al., 2000).

The centrosome consists of a pair of centrioles surrounded by pericentriolar material (PCM) from which the minus-ends of the microtubules are nucleated and anchored, and elongation occurs by distal plus-end addition of tubulin units. The γ-tubulin ring complex (γ-TuRC), which typically associates closely with both centrioles, is the most efficient nucleator of microtubules and is vital for centrosomal-directed nucleation (Hannak et al., 2002; Moritz et al., 1998; Oakley and Oakley, 1989; Schnackenberg et al., 1998; Stearns and Kirschner, 1994; Zheng et al., 1995). However, it is now widely accepted that the γ-TuRC does not have a major role in microtubule anchorage. Instead, ninein and dynactin have emerged as strong candidates for this role (Abal et al., 2002; Bornens, 2002; Lechler and Fuchs, 2007; Mogensen et al., 2000; Quintyne et al., 1999). Other proteins, including CEP135, BBS4, PCM-1, Nudel and EB1, have also been suggested to have a role in microtubule anchorage (Askham et al., 2002; Dammermann and Merdes, 2002; Guo et al., 2006; Kim et al., 2004; Ohta et al., 2002).

Ninein is a coiled-coil centrosomal protein that has a major role in microtubule minus-end anchorage and also acts as a docking site for γ-tubulin-containing complexes (Delgehyr et al., 2005; Stillwell et al., 2004). The affinity of ninein for the minus-end of microtubules is highlighted by its localisation revealed by immuno-electron microscopy to the tips of the subdistal appendages of the mother centriole, which support the minus-ends of the core radial microtubules, and to the minus-ends of both centrioles, where it colocalises with C-Nap1 (Mogensen et al., 2000; Ou et al., 2002). The role of ninein in anchorage is strongly supported by overexpression and depletion studies (Abal et al., 2002; Dammermann and Merdes, 2002). In addition, both centrioles nucleate similar numbers of microtubules by means of their γ-tubulin-associated complexes following nocodazole removal, but only the mother centriole, which possesses a higher concentration of ninein than the daughter, is able to maintain a radial array (Mogensen et al., 2000; Piel et al., 2000).

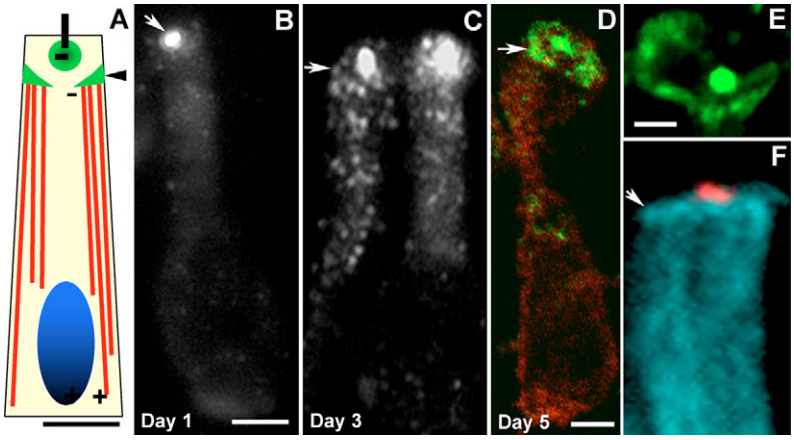

Fig. 1. Ninein speckle relocation to apical non-centrosomal sites during inner pillar cell development. (A) Schematic diagram of microtubule (red lines) and ninein (green) organisation in a typical inner pillar (IP) cell at postnatal day 5 (P5) showing microtubule minus-ends anchored at apical sites (arrowhead). (B) IP cell at P1 showing ninein mainly confined to the centrosome (arrow) at an early stage in the assembly of the apico-basal array. (C) Two IP cells at P3 with ninein at the centrosome and as distinct speckles in the cytoplasm of the apical half. Note that some of the ninein speckles are aligned in a peripheral apical ring (arrow). (D) IP cell at P5 double-labelled for dynein (red) and ninein (green), with ninein now evident at the apical peripheral ring (arrow) as well as at the centrosome. (E) Ninein peripheral ring in an IP at P6. (F) Apical region of an IP cell at P5 with microtubules (blue) forming an apico-basal array and γ-tubulin (red) concentrated at the centrosome and not evident at the apical sites (arrow). Bars, 10 μm (A-C), 5 μm (D), 2.5 μm (E,F).

Release and relocation of microtubule minus-end anchoring proteins such as ninein are likely to be central to the assembly and stabilisation of the apico-basal arrays in polarised epithelial cells. Highly polarised epithelial cells in the mammalian inner ear have proved ideal for investigating microtubule minus-end anchoring proteins and their deployment during assembly of the apico-basal arrays as nucleation and anchorage are effected at separate sites (Mogensen et al., 1997). This is particularly the case for the supporting pillar cells of the organ of Corti that assemble large non-centrosomal apico-basal arrays of several thousand microtubules during tissue morphogenesis. In these cells, γ-tubulin is concentrated at the centrosome where nucleation occurs, whereas the vast majority of the microtubule minus-ends are anchored at ninein-containing non-centrosomal apical sites (Mogensen et al., 2000; Mogensen et al., 2002). Ninein redistribution during development of the apico-basal arrays in the pillar cells suggests that ninein relocates to apical anchoring sites in a microtubule-dependent manner (Mogensen et al., 2000).

The aim of this study was to analyse the dynamics of ninein movement in epithelial cells in order to establish a model for its relocation to apical non-centrosomal anchoring sites during epithelial polarisation. Using high-resolution confocal microscopy, we show that the cytoplasmic ninein pool in cochlear pillar cells contains distinct ninein speckles, which are redeployed to apical non-centrosomal anchorage sites. Furthermore, live-cell imaging of ninein tagged with green fluorescent protein (GFP) and immuno-electron microscopy studies provide evidence for the release of ninein from the centrosome and for its subsequent microtubule-dependent motile behaviour within the cytoplasm. In addition, fluorescence recovery after photobleaching (FRAP) experiments suggest that a dynamic exchange exists between the centrosomal and cytoplasmic pools of ninein and that this movement is dependent on microtubules and not actin filaments.

Results

Cytoplasmic ninein speckles relocate to apical non-centrosomal anchoring sites during inner ear epithelial development

High-resolution confocal microscopy was used to further analyse cytoplasmic ninein at different stages during assembly of the apico-basal array in inner pillar cells of the cochlea. Inner pillar cells assemble apico-basal arrays consisting of some 3000 microtubules anchored at apical non-centrosomal peripheral sites during a 6-day post-birth period in the mouse (Fig. 1A). γ-Tubulin is concentrated at the apical centrosome throughout development and has not been detected at the apical anchoring sites, where most of the microtubule minus-ends are concentrated (Fig. 1F). In this study, we have identified a transit population of distinct non-centrosomal ninein speckles in the inner pillar cells, whose location varied with the stage of development. Ninein was concentrated at the centrosome, with only a few cytoplasmic speckles evident in the apical half of the cells, during the initial stages of assembly of the apico-basal array, when most of the microtubules are still concentrated at the centrosome (Fig. 1B) (Mogensen et al., 2000 and Fig. 4 within). However, as microtubule assembly progressed, ninein speckles became widespread throughout the apical region, and speckles started to accumulate in an apical peripheral ring by day 2-3 after birth (Fig. 1C). A distinct peripheral ring of ninein aggregates was evident by day 4-6 when the apico-basal microtubule array was close to completion and the vast majority of the minus-ends were anchored at the apical peripheral sites (Fig. 1D,E). This suggested that ninein speckles are released from the centrosome and translocated to the non-centrosomal anchoring sites. We therefore decided to investigate the dynamics of ninein and the role of microtubules in ninein speckle motility in cultured epithelial cells.

Cytoplasmic ninein speckles associate with microtubules in cultured epithelial cells

Two affinity-purified rabbit polyclonal antibodies were used to localise ninein in various cultured epithelial cells. In agreement with previous reports, the ninein antibodies were found to label the centrosome in all cell types studied, including UE-1 (Lawlor et al., 1999), PtK2, MDCKII, Caco2, FHL124 (Reddan et al., 1999), hTERT RPE (Rambhatla et al., 2002) and ARPE-19 (Dunn et al., 1996; Bouckson-Castaing et al., 1996; Mogensen et al., 2000; Piel et al., 2000) (Fig. 2A). Interestingly, ninein was also evident as distinct speckles throughout the cytoplasm in all these cells (Fig. 2A,B,E and data not shown). The authenticity of these cytoplasmic ninein speckles was verified by using siRNA ninein depletion in

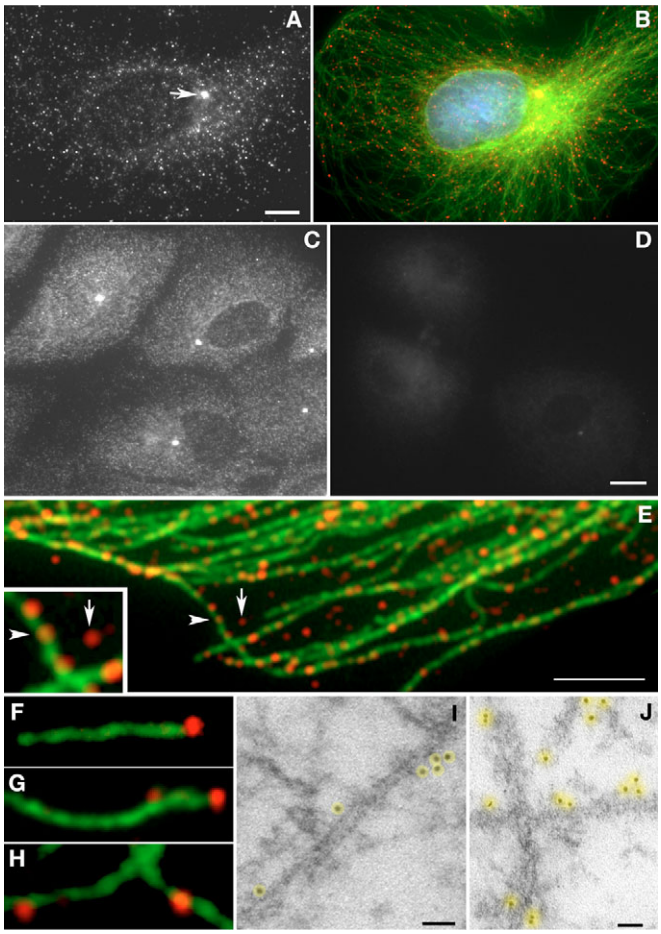

Fig. 2. Cytoplasmic ninein speckles are prominent in cultured epithelial cells. (A) PtK2 cell showing ninein at the centrosome (arrow) and throughout the cytoplasm as numerous speckles. (B) Merged image, with ninein (red) and microtubules (green). (C,D) Control (C) and siRNA-ninein-treated ARPE-19 cells labelled for ninein showing lack of cytoplasmic speckles and centrosomal staining in depleted cells (D) (images acquired using the same microscope exposure settings). (E) UE1 cell showing numerous ninein speckles (arrowhead; see also inset), which appear to be associated with microtubules. A few ninein speckles appear not to be associated with microtubules (arrow; see also inset). (F-H) Ninein speckle at the end of a free microtubule in a PtK2 (F) and a FHL124 (G) cell and along microtubules in an ARPE-19 cell (H). (I,J) Immuno-gold localisation of ninein cytoplasmic speckles in PtK2 cells. Gold particles (highlighted in yellow) are evident close to the wall of microtubules either singly or in groups of 3-4. Bars, 5 μm (A,B), 10 μm (C,D), 2 μm (E), 50 nm (I,J).

ARPE-19 cells; this resulted in loss of speckles as well as loss of centrosomal labelling (Fig. 2C,D). In all cells studied, widefield fluorescent and confocal immuno-localisation of ninein and microtubules suggested that the cytoplasmic ninein speckles associated with microtubules. Distinct ninein speckles were evident both along the length, and at the end, of microtubules, including at the ends of free microtubules (Fig. 2B,E-H). In order to verify that ninein speckles did colocalise with microtubules, the percentage of speckles observed on microtubules was calculated before and after a random shift of the microtubule image with respect to the speckle image in cells double labelled for ninein and microtubules. The percentage of speckles observed on microtubules was 81.14% (±2.66%, n=37) before image shift and 44.36% (±4.3%, n=37) after image shift. This difference is highly significant (P<0.001), and it is therefore unlikely that the ninein speckle colocalisation with microtubules was coincidental. However, some ninein speckles were evidently not associated with microtubules (Fig. 2E).

Immuno-gold labelling confirmed the centrosomal localisation of ninein and its specificity for the centriolar appendages (Fig. 6B), as previously documented (Mogensen et al., 2000). In addition, gold particles were also observed along microtubules in groups of two to four or as single particles (Fig. 2I,J). Control samples, where the primary antibody had been omitted, showed no specific labelling (data not shown). This further supported the idea that ninein speckles associate with microtubules.

Ninein speckles depend on microtubules for their distribution throughout the cytoplasm

A nocodazole assay was used to determine whether the distribution of ninein speckles in the cytoplasm was dependent on microtubules. Nocodazole caused a marked centralisation of the ninein speckles in most cells, with very few speckles remaining in the peripheral region (Fig. 3A). Some speckles were associated with nocodazole-resistant microtubules, but most were not (Fig. 3B). In order to determine whether the speckles were free in the cytosol or attached to other cytoskeletal filaments, nocodazole-treated PtK2 cells were pre-extracted with a detergent buffer (see Materials and Methods) prior to fixation and staining for ninein. This resulted in a similar centralised distribution of ninein speckles as observed for cells treated with nocodazole without detergent extraction (compare Fig. 3A with 3B). By contrast, cells treated with 2 μM latrunculin B to depolymerise the actin cytoskeleton revealed no apparent change in ninein distribution (data not shown). Nocodazole removal and microtubule regrowth led to the ninein speckles regaining their full distribution similar to that observed in untreated cells (Fig. 3D,E).

The intermediate filament network is linked to both microtubules and actin filaments and is noted for collapsing around the nucleus and withdrawing from the periphery in the absence of microtubules (Gard et al., 1997; Klymkowsky, 1982). Nocodazole treatment of PtK2 cells did cause a collapse of the keratin network in many cells. Double labelling for keratin 18 and ninein demonstrated a correlation between a central concentration of ninein and a collapsed keratin cytoskeleton in nocodazole-treated cells (Fig. 3C). In addition, ninein speckles appeared to decorate the keratin filaments (Fig. 3H). Double labelling for ninein and keratin 18 in untreated cells also suggested that some ninein speckles associated with intermediate filaments in PtK2 cells (Fig. 3F). Furthermore, immuno-gold labelling for ninein revealed gold particles along filaments of ~15 nm diameter in the electron microscope, suggestive of there being an association between ninein and intermediate filaments (Fig. 3G).

These results suggest that ninein speckle distribution throughout the cytoplasm is dependent on microtubules rather than actin filaments and that some speckles associate with the intermediate filament cytoskeleton.

Cytoplasmic ninein speckles are highly dynamic and show short- and long-range movements to and from the centrosome

Time-lapse recordings of PtK2, ARPE-19 and MDCKII cells expressing GFP-tagged ninein were used to visualise and investigate the dynamics of ninein. The GFP-ninein construct has been previously characterised (Abal et al., 2002). GFP-ninein was concentrated at the centrosome, and distinct GFP-ninein speckles were also evident in the cytoplasm, as observed for endogenous ninein in untransfected epithelial cells. Time-lapse imaging revealed that the cytoplasmic ninein speckles were highly dynamic, moving bi-directionally to and from the centrosome (Figs 4, 5; supplementary material Movies 1 and 2). Analyses of time-lapse recordings and image frames strongly suggested that some ninein speckles were released from the centrosome (Fig. 4D,E; supplementary material Movies 2-4), whereas others moved towards the centrosome (Fig. 5; supplementary material Movie 2). Two types of movement were also apparent: short and long range. The short-range movements were confined to a region relatively close to the centrosome (2-3 μm radius). This region was packed with highly dynamic ninein moving to and from the centrosome (Fig. 4A; supplementary material Movie 1). The GFP-ninein in this region appeared more string-like than that further from the centrosome (Fig. 4B,D; supplementary material Movie 4) and this was also confirmed for endogenous ninein by immuno-labelling of non-transfected cells (Fig. 4C). It is therefore unlikely to be an artefact of the GFP-ninein. The long-range speckle movements were also bi-directional, and speckles could be observed throughout the cytoplasm (Fig. 4E,F, Fig. 5A,B, supplementary material Movie 2).

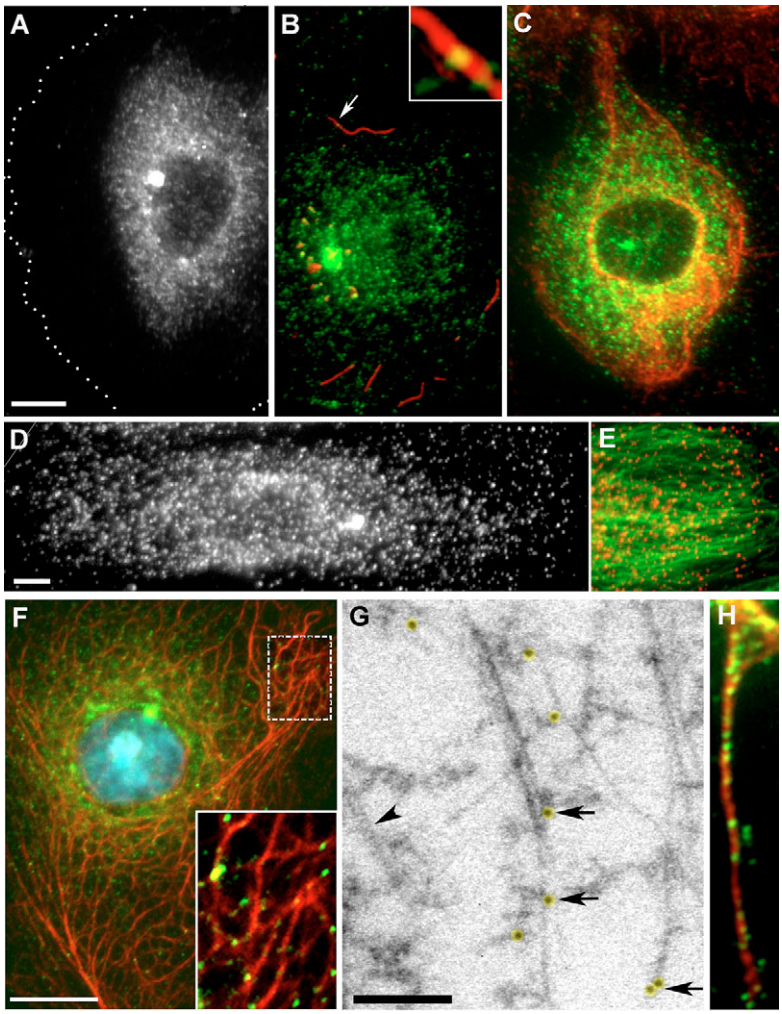

Fig. 3. Nocodazole induces centralisation of ninein speckles and reveals colocalisation with keratin filaments. (A) Nocodazole-treated PtK2 cell showing centralisation of ninein speckles (cell periphery indicated by dots). (B) PtK2 cell treated with nocodazole and 0.5% Triton X100 in PHEMO for 30 seconds prior to fixation and labelling for tubulin (red) and ninein (green) showing centralisation of the speckles and a few speckles colocalising with nocodazole-resistant microtubules (arrow, see inset). (C) PtK2 cell showing keratin filaments (K18, red) collapsed around the nucleus following nocodazole treatment. Note that the ninein (green) speckles are retained within the keratin network. (D,E) Nocodazole removal and 15 minutes regrowth results in microtubules (E) extending to the cell periphery and ninein speckles regaining their full distribution (D) (compare with Fig. 2A,B). (F) Double labelling for keratin 18 (red) and ninein (green) in an untreated cell indicates ninein speckles associated with keratin filaments. Box shows region enlarged in inset. (G) Immuno-gold labelling for ninein showing gold particles (highlighted in yellow and arrows) associated with 15 nm diameter filaments (arrowhead indicates a microtubule). (H) Keratin filaments (K18, red) from a cell treated with nocodazole and latrunculin B showing ninein (green) speckle association. Bars, 5 μm (A,B,C), 5 μm (D,E), 5 μm (F), 250 nm (G).

Average speckle velocities of 0.53 μm/second (±0.06 μm/second, n=27) away from the centrosome and 0.37 μm/second (±0.05 μm/second, n=23) towards the centrosome were apparent in PtK2 cells expressing GFP-ninein (see Materials and Methods). Tracking several ninein speckles revealed that they often used the same path (Fig. 6A,A′). Overall, analyses of speckle movements and their velocities suggested that ninein speckles were released from the centrosome and transported along microtubules by motor proteins. This was further supported by double-transfection studies using GFP-ninein and YFP–α-tubulin, which enabled visualisation of ninein speckle release from the centrosome and subsequent movement along microtubules (Fig. 6C; supplementary material Movie 5). In addition, immuno-gold localisation of ninein in the vicinity of the centrosome revealed gold particles aligned along centrosome-anchored microtubules (Fig. 6B).

Ninein speckle dynamics is inhibited by nocodazole but not latrunculin B or inhibitors of GSK3β

The data presented above strongly suggested that ninein speckle dynamics was dependent on microtubules. In order to confirm this, a nocodazole assay was used to depolymerise the microtubules in GFP-ninein-transfected PtK2 cells. All but a few stable microtubules remained following treatment with 10 μg/ml nocodazole, but full recovery occurred within ~10 minutes following nocodazole

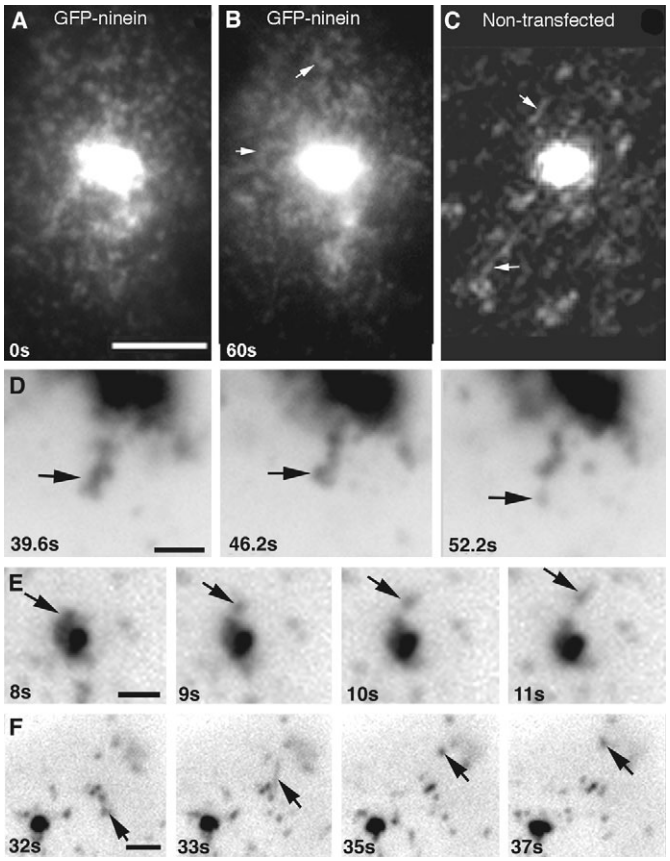

Fig. 4. GFP-ninein dynamics showing speckle release and movements away from the centrosome. (A-C) Numerous GFP-ninein speckles in the immediate environs of the centrosome in a PtK2 cell (A) were highly motile (see supplementary material Movie 1), and some had a string-like appearance [(B); arrows], which was also observed for endogenous ninein in an immuno-labelled non-transfected cell [(C); arrows]. (D) Image sequence (inverted) indicating initial release of string-like GFP-ninein followed by release of a speckle (arrows) from the centrosome in an ARPE-19 cell (see supplementary material Movie 4). (E,F) Image frames (inverted) taken from a time-lapse recording of a MDCKII cell showing a GFP-ninein speckle being released from the centrosome (E) and a speckle moving away from the centrosome (F), with arrows indicating the progress of the speckles at different time points (see supplementary material Movies 2 and 3). Time is shown in seconds (s). Bars, 2 μm.

removal (data not shown). Time-lapse imaging of the GFP-ninein speckles in nocodazole-treated cells demonstrated significantly reduced dynamics compared with non-treated cells (Fig. 7A; see supplementary material Movie 6). Nocodazole-treated cells displayed reductions of 85-90% in ninein speckle velocities, with movements away from the centrosome averaging only 0.09 μm/second (±0.05 μm/second, n=22) and towards the centrosome only 0.04 μm/second (±0.02 μm/second, n=21) (Fig. 7B).

We also tested whether the actin cytoskeleton had any significant influence. Time-lapse imaging of cells treated with 2 μM latrunculin B showed no significant effect on GFP-ninein speckle dynamics (Fig. S1A in supplementary material). Movements away from the centrosome produced an average velocity of 0.58 μm/second (±0.06 μm/second, n=36) and towards the centrosome of 0.43 μm/second (±0.04 μm/second, n=35) in cells treated with latrunculin B (Fig. 7B). Fixation of cells post imaging and labelling for microtubules and actin filaments confirmed a lack of actin filaments, whereas the radial microtubule organisation was maintained (Fig. S1B in supplementary material).

The possible involvement of glycogen synthase kinase 3β (GSK3β) in ninein speckle release and dynamics was also investigated. Phosphorylation by polo-like kinase 1 (Plk1) has been shown to be responsible for the release of ninein-like protein (Nlp) from the centrosome but this is not the case for ninein (Casenghi et al., 2005). However, GSK3β, which is present at the centrosome, has been reported to phosphorylate ninein (Hong et al., 2000a; Hong et al., 2000b; Howng et al., 2004) and could potentially influence its association with the centrosome. We therefore investigated the affect of GSK3β inhibition on ninein release from the centrosome. GFP-ninein-expressing cells were treated with one of three different inhibitors of GSK3β (LiCl, SB415286, SB216763; see Materials and Methods) prior to time-lapse imaging. None of the three inhibitors of GSK3β appeared to affect ninein release or cause any significant reduction in its dynamics, suggesting that GSK3β is not responsible for ninein release from the centrosome (Fig. S2 in supplementary material).

FRAP analyses suggest microtubule-dependent centrosomal GFP-ninein recovery

The time-lapse studies indicated that ninein speckles were actively transported to the centrosome along microtubules (Fig. 5; see supplementary material Movie 2). We decided to explore further the recruitment of ninein to the centrosome by using FRAP. FRAP analyses were carried out in PtK2 cells expressing GFP-ninein by using a Zeiss LSM 510 META confocal scanning microscope, and the centrosome was selected for photobleaching (see Materials and Methods). In the presence of an intact microtubule cytoskeleton, almost complete (average 98.48±1.52%, n=5) fluorescent recovery of centrosomal ninein occurred within 2.5 minutes following photobleaching (Fig. 8A,C,D). However, FRAP analysis of centrosomes in nocodazole-treated cells showed little or no recovery (average 23.83±3.68%, n=6) after 4 minutes or even after extended time periods of up to 10 minutes (Fig. 8B-D). These FRAP studies suggest that there is a dynamic exchange between the cytoplasmic and centrosomal pools of ninein and that microtubules are required for efficient ninein transport to the centrosome.

Ninein speckles localise to apical anchoring sites in polarised MDCKII cells

Ninein deployment was also investigated in polarised MDCKII cells; ninein was present at the centrosome and as speckles in the cytoplasm, as also observed in non-polarised epithelial cells. However, in single optical sections through the apical region of polarised cells, a distinct punctate pattern of ninein was evident at the cell periphery (Fig. 9A). A marked accumulation of ninein within the apical cell peripheral region became apparent in lateral and apical views of 3D reconstructions of polarised MDCKII cells (Fig. 9B,G,H). Polarised MDCKII cells, like the pillar cells, contain an apico-

basal array of microtubules, with most of the minus-ends anchored at non-centrosomal apical sites (Bacallao et al., 1989; Meads and Schroer, 1995; Musch, 2004). 3D reconstructions of the microtubule organisation in polarised MDCKII cells revealed that most of the apico-basal microtubules form a tube, with the minus-ends organised in a peripheral ring at the apex (data not shown). So, even though there are significantly (~tenfold) fewer microtubules in polarised MDCKII cells compared with inner pillar cells, a peripheral ninein ring was again evident at the non-centrosomal microtubule minus-end anchoring sites, as observed in the pillar cells (Fig. 9H).

The peripheral location of the ninein ring suggested that it was within the domain of adherens junctions. E-cadherin is responsible for cell-cell adhesion, and its cytoplasmic tail interacts with β-catenin. Double labelling for ninein and either E-cadherin or β-catenin revealed no significant colocalisation with E-cadherin but considerable colocalisation at the cell periphery with β-catenin (Fig. 9C; see also Fig. S3 in supplementary material). Colocalisation of ninein and β-catenin was confirmed using both the Zeiss and Volocity classification programs (Fig. 9D-F). Similar colocalisation was also observed in supporting Kollikers cells of the cochlea (data not shown). However, a direct physical interaction between ninein and β-catenin could not be confirmed by co-immunoprecipitation.

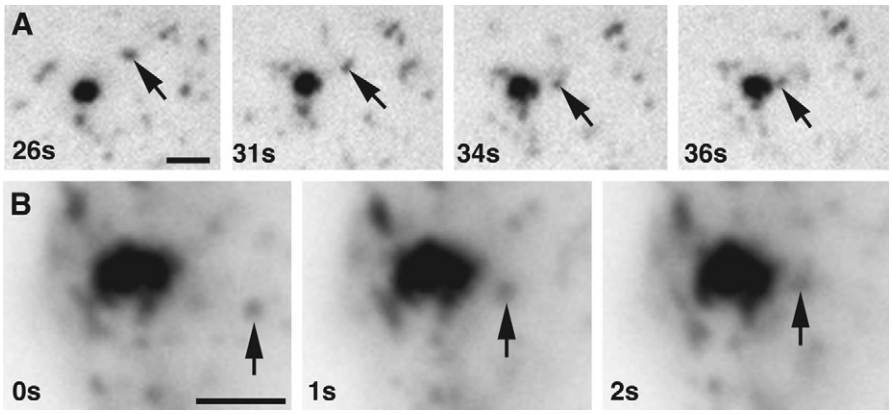

Fig. 5. GFP-ninein speckle movements towards the centrosome. (A) Image sequence (inverted) taken from the same time-lape recording as Fig. 4E,F showing a MDCKII cell expressing GFP-ninein, with a speckle (arrow) moving towards the centrosome (see supplementary material Movie 2). (B) A speckle (arrow) moving towards the centrosome in a GFP-ninein-expressing ARPE-19 cell. Time is shown in seconds (s). Bars, 2 μm.

Discussion

The centrosomal protein ninein acts as a microtubule minus-end anchoring protein at the centrosome in cells deploying a radial microtubule array and at apical sites in polarised epithelial cells, which assemble non-centrosomal apico-basal arrays. Functional inhibition studies including microinjection of antibodies against ninein (Ou et al., 2002) and siRNA depletion (Dammermann and Merdes, 2002), which result in loss of centrosomal focus, and ninein overexpression, which enhances centrosomal anchorage (Abal et al., 2002), all provide strong evidence for a role for ninein in anchorage. However, little is known about the mechanisms responsible for ninein relocation during epithelial differentiation, and yet ninein is clearly central to microtubule reorganisation in polarised epithelial cells.

Ninein speckles associate with microtubules and intermediate filaments and require microtubules for their distribution throughout the cytoplasm

Ninein was observed not only at the centrosome but also within the cytoplasm as distinct speckles in several epithelial cell types, suggesting that these speckles are a general feature of epithelial cells. Cytoplasmic diffuse ninein has previously been observed in developing cochlear epithelial cells (Mogensen et

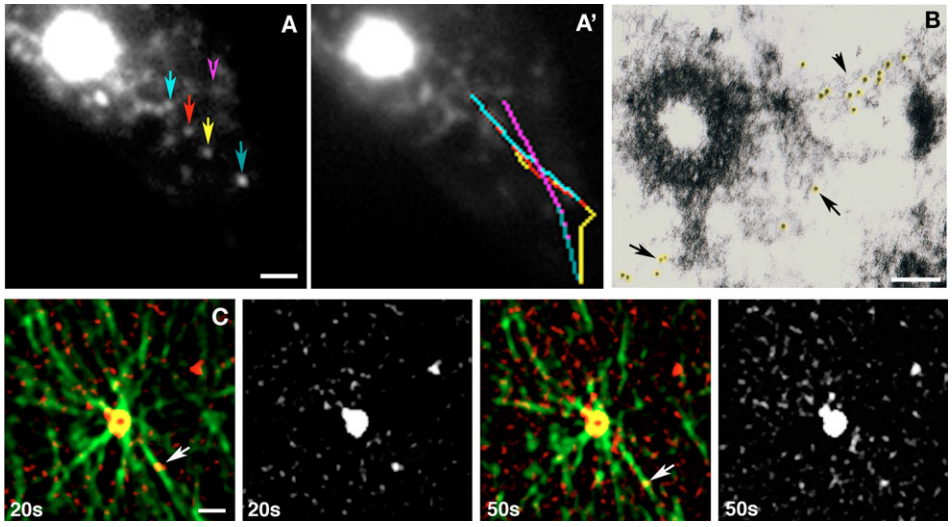

Fig. 6. GFP-ninein speckles travel along microtubules. (A,A′) Tracking of GFP-ninein speckles moving away from the centrosome over successive frames reveals several speckles following the same path. The speckles are indicated by a coloured arrow in (A), and their paths are shown by the corresponding coloured lines in (A′). (B) Immuno-gold labelling for ninein in the centrosomal region showing gold particles (highlighted in yellow) along the wall of a microtubule (arrowhead) anchored to one of the subdistal appendages of the mother centriole. Also note gold particles associated with the subdistal appendices (arrows). (C) Time-lapse frames of the centrosomal region of a PtK2 cell expressing GFP-ninein (red) and YFP–α-tubulin (green) (see supplementary material Movie 5). GFP-ninein speckles appear associated with the radiating microtubules (arrows). The frames show distinct changes in ninein speckle distribution over time. Time is shown in seconds (s). Bars, 1 μm (A,A′), 100 nm (B), 2 μm (C).

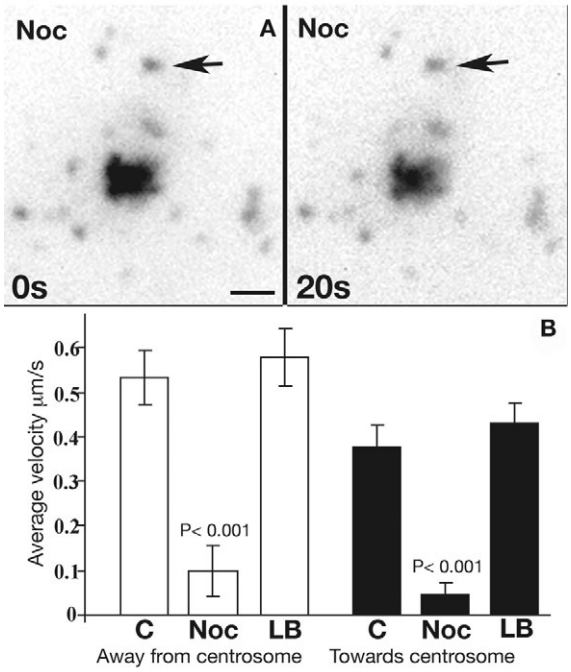

Fig. 7. Microtubules are required for GFP-ninein speckle dynamics. (A) Two image frames (inverted) of the centrosome region taken from a time-lapse series of a GFP-ninein-expressing PtK2 cell treated with nocodazole (see supplementary material Movie 6) showing no positional changes in the speckles. The arrow highlights one of the speckles. Time is shown in seconds (s). Scale bar: 2 μm. (B) Quantitative analyses of GFP-ninein speckle velocities for movements away from the centrosome in control (C) PtK2 cells (0.53±0.06 μm/second, n=27) and in PtK2 cells pre-treated with nocodazole (NOC) (0.09±0.05 μm/second, n=22) or latrunculin B (LB) (0.58±0.06 μm/second, n=36) and towards the centrosome in control (C) (0.37±0.05 μm/second, n=23), nocodazole (NOC) (0.04±0.02 μm/second, n=21) and latrunculin B (LB) treated (0.43±0.04 μm/second, n=35) cells. The results show that only nocodazole is able to significantly (P<0.001) inhibit ninein speckle movements both to and from the centrosome, indicating that microtubules and not actin filaments are required for speckle dynamics.

al., 2000), and ninein speckles have been reported in neurons (Baird et al., 2004). These are both systems that assemble large non-centrosomal microtubule arrays. However, what role the ninein speckles serve in undifferentiated epithelial cells and neurons is currently not known. Interestingly, ninein was observed at the ends of free microtubules in some epithelial cells in this study, and it is tempting to speculate that it could have a role in minus-end capping and stabilisation of non-centrosomal microtubules. This is supported by microinjection of antibodies against ninein, which not only caused the release of microtubules but also their subsequent depolymerisation (D.K.M., J.M.C. and M.M.M., unpublished). It is also of note that ninein speckles have been reported to be highly abundant in neurons, which contain predominantly non-centrosomal microtubules (Baird et al., 2004). Alternatively or additionally, these speckles might represent a cytoplasmic store in dynamic exchange with the centrosome, as found for other core centrosomal components including γ-tubulin and centrin (Moudjou et al., 1996; Paoletti et al., 1996). This is supported by our FRAP data. The cytoplasmic ninein speckles might also represent an intermediate stage in the redistribution process, which requires final signals from developing cell junctions in order to progress to the anchoring sites. For example, in suprabasal cells of the epidermis, desmoplakin is required for the recruitment of ninein to desmosomes, with ninein remaining centrosomal and cytoplasmic in desmoplakin knockouts (Lechler and Fuchs, 2007).

Immuno-fluorescence and immuno-electron microscopy as well as drug (nocodazole and latrunculin B) treatments strongly suggest that ninein speckles associate with and depend on microtubules for their distribution throughout the cytoplasm. Ninein speckles were observed to decorate microtubules along their length in all the cells studied. An association with keratin filaments was also observed in PtK2 cells, whereas there was no apparent association with actin filaments. So far, no microtubule-binding domain has been identified for ninein, but an interaction with the p150^{glued}, p50 and Arp1 subunits of the dynactin complex has been reported (Casenghi et al., 2005). Ninein speckles could therefore bind to microtubules via the dynein-dynactin complex. Similarly, ninein speckles could bind indirectly to intermediate filaments by means of dynein, which has also been shown to associate with intermediate filaments (Helfand et al., 2002).

Nocodazole induced a centripetal localisation of the ninein speckles in many cells, but microtubule regrowth re-established their distribution throughout the cytoplasm. Latrunculin B, by contrast, caused no apparent change in ninein distribution. Interestingly, the few nocodazole-treated cells that still showed speckles throughout the cytoplasm retained a fully extended keratin network. The centralisation of the speckles is thus likely to be due to ninein speckle association with a peripherally withdrawn and collapsed keratin filament network. Intermediate filaments are linked to both microtubules and actin filaments and are particularly dependent on microtubules for their distribution (Gard et al., 1997; Klymkowsky, 1982). Microtubules are clearly required for ninein speckle distribution throughout the cytoplasm, but intermediate filaments might also influence their deployment.

Ninein speckles are released from the centrosome and move bi-directionally along microtubules

These studies provide visual evidence for the release of ninein speckles from the centrosome and for their subsequent bi-directional movements within the cytoplasm. Two types of movements were observed, one short range, pericentrosomal with string-like ninein, and the other long range, involving extensive movements to and from the centrosome by distinct speckles. The string-like or short filaments of ninein observed close to the centrosome might represent an intermediate stage in the ninein release process. Interestingly, ultrastructural analyses of centrosomal ninein aggregates have revealed a network of filaments and nodes (Abal et al., 2002). How ninein speckles are released from the centrosome is not known, but it is likely that phosphorylation is involved. For example, phosphorylation of Nlp by Plk1 is responsible for its displacement from the centrosome at G_2-M phase (Casenghi et al., 2005). Plk1 does not phosphorylate ninein (Casenghi et al., 2005), but GSK3β, which is present at the centrosome, interacts with the C-terminus of ninein and phosphorylates ninein (Hong et al., 2000a; Hong et al., 2000b; Howng et al.,

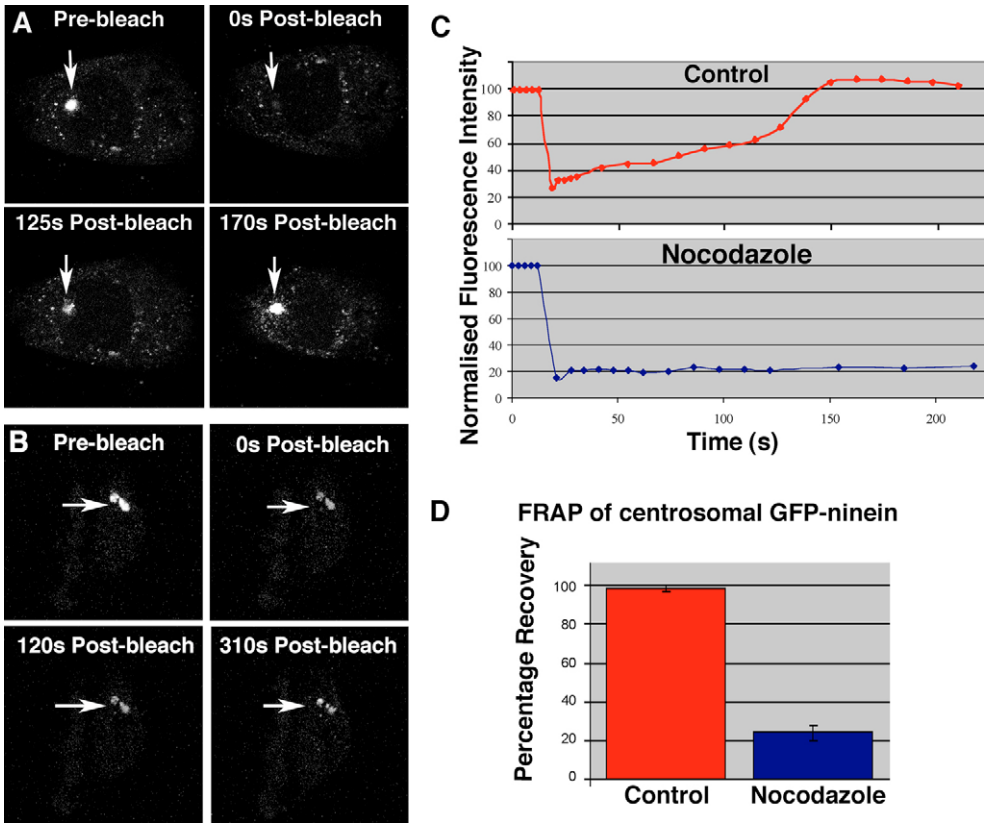

Fig. 8. FRAP analyses of GFP-ninein at the centrosome in PtK2 cells. (A) Images from a time-lapse recording showing recovery of GFP-ninein at the centrosome following photobleaching (arrows). (B) Images from a time-lapse recording of a cell pre-treated with nocodazole showing no significant recovery at the centrosome (arrows) following photobleaching. (C) Graphs depicting the fluorescence intensity during recovery following photobleaching of the control cell in A (red line) and the nocodazole-treated cell in B (blue line). The fluorescence intensity at the centrosome following photobleaching was normalised to that prior to photobleaching. (D) Histogram comparing percentage centrosomal GFP-ninein fluorescence recovery 4 minutes after photobleaching in control (red; 98.48±1.52%, *n*=5) and nocodazole (blue; 23.83±3.68%, *n*=6) treated cells.

2004). However, three different inhibitors of GSK3β used in this study did not cause any significant reduction in ninein dynamics or release from the centrosome, suggesting that GSK3β is not responsible for ninein release.

Several lines of evidence provide strong support for ninein speckle dynamics being dependent on microtubules. Analyses of GFP-ninein speckle release and movements from the centrosome showed several speckles following the same tracks, and double-transfection studies with GFP-ninein and YFP–α-tubulin suggested that the speckles moved along microtubules. In addition, immuno-electron microscopy localised ninein to centrosomally anchored microtubules. Furthermore, nocodazole greatly reduced all speckle movements, whereas latrunculin B had no significant affect. The bi-directional speckle movements along microtubules are most likely mediated by motor proteins. The estimated average ninein speckle velocity away from the centrosome was 0.53 μm/second in PtK2 cells, which is within the range of kinesin motors (0.1-1.5 μm/second). However, which kinesin motor is responsible for ninein speckle movement towards the cell periphery is unknown but warrants future investigation. However, the estimated average speckle velocity for movements towards the centrosome was 0.37 μm/second in PtK2 cells, which is less than that expected for dynein (0.5-2.0 μm/second). Analyses of speckle dynamics in the PtK2 cells did include speckles displaying brief periods of pausing, and it is likely that these pauses account for the relatively low average speckle velocity. Furthermore, velocity calculations based only on moving speckles (i.e. excluding pauses) in MDCKII cells were 0.81 μm/second away from and 0.83 μm/second towards the centrosome (Fig. S2), which falls within the expected ranges for kinesin and dynein.

The observation of bi-directional movements of ninein speckles to and from the centrosome suggested an exchange between centrosomal and cytoplasmic ninein. This was supported by the FRAP studies, which revealed that 60-90% of ninein was exchanged within 2.5 minutes. Pre-treatment with nocodazole resulted in no significant recovery following photobleaching, suggesting that ninein transport to the centrosome is dependent on microtubules. Dynein has previously been shown to be required for centrosomal targeting of ninein, with dynein inhibition by excess of either p50 (dynamitin/dynactin subunit) or p150^{Glued} CC1 causing centrosomal depletion of ninein (Casenghi et al., 2005; Dammermann and Merdes, 2002). We have also shown that overexpression of p150^{Glued} CC1 causes ninein depletion at the centrosome as well as disorganised microtubules lacking centrosomal focus (data not shown). PCM-1 and bicaudal-D (BICD) have both been reported to be involved in the transport of ninein to the centrosome in a dynein-dependent manner (Dammermann and Merdes, 2002; Fumoto et al., 2007). However, the reported interaction between ninein and the dynein-dynactin complex suggests that at least a fraction of ninein moves independently of PCM-1 and BICD.

Most importantly, these studies of dynamics provide evidence for epithelial cells possessing the mechanical means for the release and translocation of ninein from the centrosome to non-centrosomal anchoring sites.

Centrosomal ninein is released and relocated to junction-associated apical sites during epithelial polarisation

These studies have identified distinct ninein speckles in supporting cochlear epithelial cells and provided further

evidence for the redeployment of ninein to the apical anchoring sites during normal tissue morphogenesis in situ. In addition, we show for the first time that ninein is similarly redeployed to apical peripheral anchoring sites following in vitro polarisation of MDCKII cells. We also show that cytoplasmic ninein speckles are a general feature of epithelial cells and that they are highly dynamic, displaying microtubule-dependent movements within the cytoplasm.

Interestingly, we report extensive colocalisation of ninein and β-catenin at cell junctions in polarised MDCKII and supporting cochlear cells. This suggests that ninein accumulates at and the non-centrosomal anchoring sites form in close proximity to adherens junctions. Expression of cadherin junction components has been reported to increase microtubule minus-end stability, and β-catenin has been suggested to mediate this link (Chausovsky et al., 2000). The data presented in this study thus suggest a possible link between ninein and β-catenin and support a role for adherens junctions and β-catenin in the establishment of non-centrosomal apico-basal microtubule arrays in polarised epithelial cells. We therefore propose that ninein speckles are released from the centrosome and transported along microtubules by plus-end-directed kinesin motors to apical non-centrosomal anchoring sites. In addition, we suggest that the anchoring sites form in association with adherens junctions during assembly of the apico-basal microtubule arrays. These studies clearly also highlight the vital role that ninein dynamics and redistribution play in microtubule reorganisation during epithelial polarisation and differentiation.

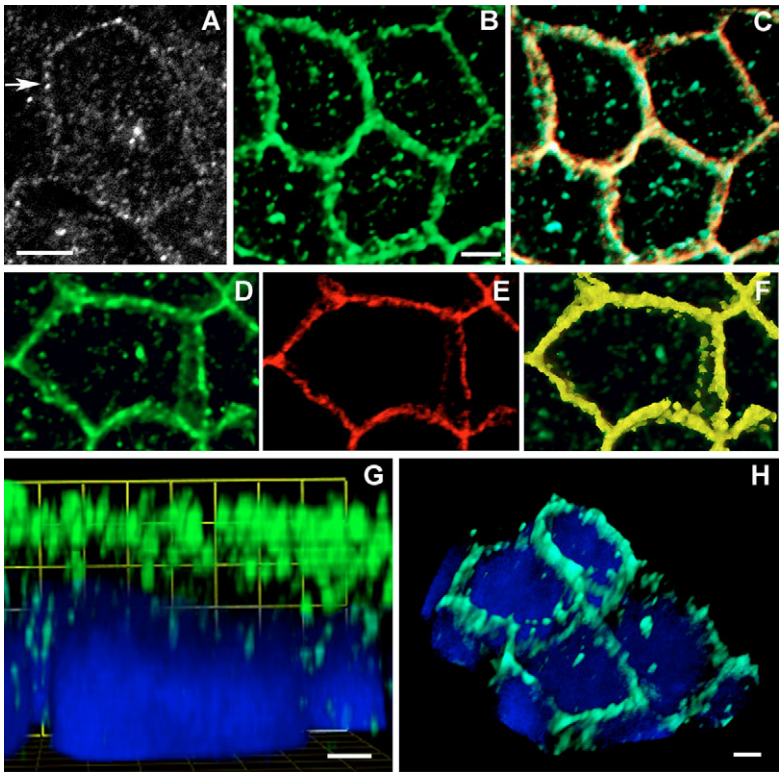

Fig. 9. Ninein localisation in polarised MDCKII cells. (A) Single confocal optical section through the apical region of a polarised MDCKII cell, with ninein at the centrosome, as speckles in the cytoplasm, and at the cell periphery where it forms a distinct punctate pattern (arrow). (B) Apical view of a 3D reconstruction (based on confocal optical sections) of three polarised cells showing ninein at the centrosome and accumulated within a peripheral ring at the location of the anchoring sites. (C) Merged image, with ninein (green) and β-catenin (red), showing regions of substantial colocalisation (yellow) at the cell periphery. (D-F) Regions of colocalisation analysed using Volocity (Improvision) software, with (F) indicating regions with strong colocalisation (yellow). (G) Lateral view of a 3D reconstruction from a confocal Z stack of a polarised cell showing the distinct apical localisation of ninein (green). The nucleus is labelled with DAPI (blue). (H) Rotated image showing an oblique view of a 3D reconstruction of a group of four cells, with ninein (green) at the centrosomes and concentrated within apical peripheral rings. The nucleus is labelled with DAPI (blue). Bars, 5 μm (A,D,E,F), 5 μm (B,C), 2 μm (G,H).

Materials and Methods

Antibodies

Two rabbit anti-ninein antibodies generated against the same GST fusion peptide [Pep3, sequence 952-1227 (Bouckson-Castaing et al., 1996); gift from M. Bornens, Institute Curie, Paris, France] were used in these studies. One was a gift from M. Bornens and the other was newly generated, affinity purified and tested for specificity. The ninein antibodies were used at 1:1000 (0.1 mg/ml). Control experiments involving pre-incubation of the antibody with the Pep3 peptide resulted in no detectable labelling. Furthermore, siRNA depletion of ninein in ARPE-19 cells (human cell line, using two sequences: sense CGGUACAAUGAGUGUAGAATT and antisense: UUCUACACUCAUUGUACC-GTC from Ambion and sense: GGAAGACCUAAGAAAUGU and antisense: UACAUUUCUUAGGUCUUCC from Qiagen) was used to verify the specificity of the ninein antibody. Cells were transfected with the siRNAs twice, with an interval of 48 hours between transfections and for a total of 96 hours and the cells were fixed and labelled with the ninein antibody. A combination of the two sequences produced the best depletion results. A scramble sequence was used as control.

Monoclonal antibodies against α-tubulin (Sigma), β-catenin and E-cadherin (BD Transduction Laboratories) and rabbit polyclonal for γ-tubulin (Sigma) were used at 1 in 1000. Monoclonal antibody against keratin 18 (LE65) was used undiluted. F-actin was labelled using rhodamine-conjugated phalloidin (Molecular Probes) at 1:200. All secondary antibodies used for immuno-fluorescence were conjugated to AlexaFluor 488, 568 or 594 (Molecular Probes) and used at a dilution of 1:1000.

Cell culture and transfection

MDCKII (Madin-Darby Canine kidney) and FHL124 (lens epithelial, gift from G. Duncan, University of East Anglia, Norwich, UK) cells were cultured in DMEM (Invitrogen) with 10% (v/v) FCS (Invitrogen) and 1% (v/v) L-Glutamine (Invitrogen) at 37°C with 5% CO_2. PtK2 (potaroo kidney epithelial) cells and the two retinal pigmented epithelial cell lines ARPE-19 and hTERT RPE (both gifts from J. Sanderson, University of East Anglia, Norwich, UK) were cultured in DMEM diluted 1:1 with Hams NUT F12 (Invitrogen) with 10% FCS and 1% L-glutamine. UE-1 (inner ear cell line, gift from M. Holley, University of Sheffield, UK) cells were cultured in MEM containing Earl's salts Glutamax (Invitrogen) and γ-Interferon (Sigma, 50 U/ml) at 33°C with 5% CO_2. MDCKII cells were polarised on uncoated 0.4 μm polycarbonate membrane filters (Nunc) in DMEM with 5% FCS for 3-4 days at 37°C.

Cells were transfected at 60-70% confluence using FuGene VI (Roche) and incubated for 12-16 hours at 37°C. In double transfection experiments, both plasmid DNAs were mixed at a 1:1 ratio. Cells for live imaging were grown on 40 mm diameter cover slips for use in a POC-R chamber. The GFP-ninein construct was a gift from M. Bornens [Institute Curie, France (Abal et al., 2002)]. The EYFP-tubulin construct was obtained by cloning full-length cDNA sequence of α-tubulin into the *Xho*I and *Bam*HI sites of the pEYFP-C1 vector (Clontech).

Immuno-fluorescence labelling of cultured and isolated pillar cells

Cultured cells and isolated cochlear pillar cells [dissected as described previously; (Mogensen et al., 2002)] were fixed in cold (–20°C) 90% methanol/10% MES (100 mM MES, 1 mM EGTA, 1 mM $MgSO_4$ at pH 6.9, Sigma) for 4 minutes, rehydrated in 1% goat serum in PBS and detergent treated with 1% NP40 in PBS for 4 minutes, blocked in 10% goat serum in PBS and incubated in primary antibodies for 30-90

minutes followed by secondary antibodies for 30 minutes. Cells labelled with phalloidin were fixed with 4% paraformaldehyde in PBS and extracted in 1% NP40 in PBS, and cells labelled for both actin and microtubules were fixed in 3.7% paraformaldehyde in PHEMO buffer (68 mM PIPES, 25 mM HEPES, 15 mM EGTA and 3 mM $MgCl_2$) with 0.5% glutaraldehyde and 0.5% Triton X-100 (Sigma) for 10 minutes and quenched with 50 nM NH_4Cl in PBS for 10 minutes and labelled as above.

Fluorescent images were recorded using either a Zeiss Axiovert 200M with a Zeiss AxioCam camera and Axiovision software or a Zeiss LSM 510 META confocal microscope with associated software. Z-stacks were generated from optical sections taken at 0.2 μm intervals, and Volocity (Improvision) software program was used for 3D reconstruction. The Volocity classification and Zeiss LSM510 META software programs were used to analyse colocalisation and determine signal overlap. Digital image files were transferred to Photoshop CS2 for image handling.

Immuno-gold labelling and TEM

PtK2 cells were fixed in 4% paraformaldehyde and 0.1% glutaraldehyde in cytoskeletal buffer (10 mM MES, 150 mM NaCl, 5 mM EGTA, 5 mM $MgCl_2$, 5 mM glucose at pH 6.9) with 0.3% TritonX-100, blocked in 10% goat serum in PBS, incubated with ninein antibody overnight at 4°C, washed and incubated in protein-A conjugated to 8 nm gold particles, post-fixed in 2.5% glutaraldehyde in cacodylate buffer (0.1 M sodium cacodylate, 2.0 M calcium chloride) for 40 minutes followed by 1% osmium tetroxide for 40 minutes, processed for electron microscopy and imaged using a JOEL 200 TEM.

Drug treatments

Cells were treated with 10 μg/ml nocodazole (Sigma) for 60 minutes on ice followed by 2 hours at 37°C for microtubule depolymerisation and fixed or washed several times in cold medium prior to regrowth at 37°C. Latrunculin B (Sigma) at 2 μM was used for actin depolymerisation, and cells were incubated at 37°C for 30 minutes. Cell extraction was carried out with 0.5% Triton X-100 in PHEMO for 30 seconds after nocodazole treatment but before fixation.

GFP-ninein-expressing ARPE-19 and MDCKII cells were treated with one of three different inhibitors of GSK3β (20 mM LiCl, 1 μM SB216763 or 10 μM SB415286) for 2-24 hours prior to time-lapse analyses (Coghlan et al., 2000; Streets et al., 2006). Control cells were treated with 0.2% DMSO for 24 hours and behaved as untreated cells.

Live cell imaging and analyses

Cells expressing GFP-ninein or GFP-ninein and YFP–α-tubulin were maintained in a POC-R chamber on a heated stage at 37°C in phenol-red free medium (Invitrogen) for live recording. Images were captured using a 63× 1.4 NA objective on a fully automated Zeiss Axiovert 200M using a Zeiss AxioCam and Axiovision software. For double transfections of GFP-ninein and YFP–α-tubulin, filter sets JP3 (Chroma) were used in conjunction with Delta Vision software (Applied Precision Inc.) to distinguish between the two fluorochromes. Images were captured on a Micromax CCD camera (Roper Scientific, Trenton, NJ) camera and deconvolved using softWoRx (Applied Precision Inc.). Cells destined for nocodazole treatment were treated as described above and then imaged with 10 μg/ml nocodazole added to the POC-R chamber.

Ninein speckle velocities were calculated by tracking individual speckles over time (1-2 second time intervals). One Way Analysis of Variance (ANOVA) followed by Tukey's post hoc analysis was used to determine significance at the 5% level. An overall average speckle velocity was calculated based on all trackable speckles, including speckles displaying brief periods of pausing in GFP-ninein-expressing control-, nocodazole- and latrunculin-B-treated PtK2 cells. However, for analyses of the affect of GSK3β inhibitors on ninein dynamics in MDCKII cells, only moving speckles were used for velocity estimations.

The colocalisation of ninein speckles with microtubules was verified by calculating the percentage of speckles observed on microtubules before and after a random shift of the microtubule image with respect to the speckle image in two cells double-labelled for ninein and microtubules. The percentage of speckles located either on or off a microtubule was calculated within 37 areas in two cells and the significance was determined using a *t* test.

FRAP analyses

FRAP data were acquired using the Zeiss LSM 510 META confocal. Images were collected prior to photobleaching as a measure of the original intensity. The Argon/Ion laser (488) was used at 4% intensity for image acquisitions. The centrosome in GFP-ninein transfected PtK2 cells was selected using the LSM imaging software and photobleached using the Argon/Iron laser at 30-40 iterations at 100% intensity. Images were recorded post-bleaching during centrosomal recovery. The centrosomal GFP recovery was determined by measuring the signal intensity of the photobleached region over time, using normal imaging parameters set prior to bleaching.

We are very grateful for help with the live-cell imaging from Paul Thomas (Henry Wellcome Laboratory for Cell Imaging at the University of East Anglia, UK), for EM assistance from John James (Electron Microscope Facility, University of Dundee, UK) and Richard Evans-Gowing (University of East Anglia, UK) and for help with tissue culture from Alba Warn and Diane Alden (University of East Anglia, UK). We would also like to thank Michel Bornens (Institute Curie, France) for the kind gifts of ninein antibody, GFP-ninein construct and GST-pep3 construct, and Matthew Holley (University of Sheffield, UK) for the UE-1 inner ear cell line. This work was supported by The Wellcome Trust (Grant 067816/Z/02/Z to M.M.M. and J.M.C.), The Anatomical Society of Great Britain and Ireland (Studentship support to D.K.M.), BBSRC (Grant BB/D012201\1 to M.M.M. and G.B.), Big C Appeal (Studentship support to J.K.), Zeiss Microscope Division, UK (to M.M.M.) and Cancer Research UK (Grant C26/A1461 to E.B.L.).

References

Abal, M., Piel, M., Bouckson-Castaing, V., Mogensen, M., Sibarita, J. B. and Bornens, M. (2002). Microtubule release from the centrosome in migrating cells. *J. Cell Biol.* **159**, 731-737.

Askham, J. M., Vaughan, K. T., Goodson, H. V. and Morrison, E. E. (2002). Evidence that an interaction between EB1 and p150(Glued) is required for the formation and maintenance of a radial microtubule array anchored at the centrosome. *Mol. Biol. Cell* **13**, 3627-3645.

Bacallao, R., Antony, C., Dotti, C., Karsenti, E., Stelzer, E. H. and Simons, K. (1989). The subcellular organization of Madin-Darby canine kidney cells during the formation of a polarized epithelium. *J. Cell Biol.* **109**, 2817-2832.

Baird, D. H., Myers, K. A., Mogensen, M., Moss, D. and Baas, P. W. (2004). Distribution of the microtubule-related protein ninein in developing neurons. *Neuropharmacology* **47**, 677-683.

Bornens, M. (2002). Centrosome composition and microtubule anchoring mechanisms. *Curr. Opin. Cell Biol.* **14**, 25-34.

Bouckson-Castaing, V., Moudjou, M., Ferguson, D. J., Mucklow, S., Belkaid, Y., Milon, G. and Crocker, P. R. (1996). Molecular characterisation of ninein, a new coiled-coil protein of the centrosome. *J. Cell Sci.* **109**, 179-190.

Bre, M. H., Kreis, T. E. and Karsenti, E. (1987). Control of microtubule nucleation and stability in Madin-Darby canine kidney cells: the occurrence of noncentrosomal, stable detyrosinated microtubules. *J. Cell Biol.* **105**, 1283-1296.

Bre, M. H., Pepperkok, R., Hill, A. M., Levilliers, N., Ansorge, W., Stelzer, E. H. and Karsenti, E. (1990). Regulation of microtubule dynamics and nucleation during polarization in MDCK II cells. *J. Cell Biol.* **111**, 3013-3021.

Casenghi, M., Barr, F. A. and Nigg, E. A. (2005). Phosphorylation of Nlp by Plk1 negatively regulates its dynein-dynactin-dependent targeting to the centrosome. *J. Cell Sci.* **118**, 5101-5108.

Chausovsky, A., Bershadsky, A. D. and Borisy, G. G. (2000). Cadherin-mediated regulation of microtubule dynamics. *Nat. Cell Biol.* **2**, 797-804.

Coghlan, M. P., Culbert, A. A., Cross, D. A., Corcoran, S. L., Yates, J. W., Pearce, N. J., Rausch, O. L., Murphy, G. J., Carter, P. S., Roxbee Cox, L. et al. (2000). Selective small molecule inhibitors of glycogen synthase kinase-3 modulate glycogen metabolism and gene transcription. *Chem. Biol.* **7**, 793-803.

Dammermann, A. and Merdes, A. (2002). Assembly of centrosomal proteins and microtubule organization depends on PCM-1. *J. Cell Biol.* **159**, 255-266.

Delgehyr, N., Sillibourne, J. and Bornens, M. (2005). Microtubule nucleation and anchoring at the centrosome are independent processes linked by ninein function. *J. Cell Sci.* **118**, 1565-1575.

Dunn, K. C., Aotaki-Keen, A. E., Putkey, F. R. and Hjelmeland, L. M. (1996). ARPE-19, a human retinal pigment epithelial cell line with differentiated properties. *Exp. Eye Res.* **62**, 155-169.

Fumoto, K., Hoogenraad, C. C. and Kikuchi, A. (2007). GSK-3beta-regulated interaction of BICD with dynein is involved in microtubule anchorage at centrosome. *EMBO J.* **25**, 5670-5682.

Gard, D. L., Cha, B. J. and King, E. (1997). The organization and animal-vegetal asymmetry of cytokeratin filaments in stage VI Xenopus oocytes is dependent upon F-actin and microtubules. *Dev. Biol.* **184**, 95-114.

Guo, J., Yang, Z., Song, W., Chen, Q., Wang, F., Zhang, Q. and Zhu, X. (2006). Nudel contributes to microtubule anchoring at the mother centriole and is involved in both dynein-dependent and -independent centrosomal protein assembly. *Mol. Biol. Cell* **17**, 680-689.

Hannak, E., Oegema, K., Kirkham, M., Gonczy, P., Habermann, B. and Hyman, A. A. (2002). The kinetically dominant assembly pathway for centrosomal asters in Caenorhabditis elegans is gamma-tubulin dependent. *J. Cell Biol.* **157**, 591-602.

Helfand, B. T., Mikami, A., Vallee, R. B. and Goldman, R. D. (2002). A requirement for cytoplasmic dynein and dynactin in intermediate filament network assembly and organization. *J. Cell Biol.* **157**, 795-806.

Hong, Y. R., Chen, C. H., Chang, J. H., Wang, S., Sy, W. D., Chou, C. K. and Howng, S. L. (2000a). Cloning and characterization of a novel human ninein protein that interacts with the glycogen synthase kinase 3beta. *Biochim. Biophys. Acta* **1492**, 513-516.

Hong, Y. R., Chen, C. H., Chuo, M. H., Liou, S. Y. and Howng, S. L. (2000b). Genomic organization and molecular characterization of the human ninein gene. *Biochem. Biophys. Res. Commun.* **279**, 989-995.

Howng, S. L., Hsu, H. C., Cheng, T. S., Lee, Y. L., Chang, L. K., Lu, P. J. and Hong, Y. R. (2004). A novel ninein-interaction protein, CGI-99, blocks ninein phosphorylation by GSK3beta and is highly expressed in brain tumors. *FEBS Lett.* **566**, 162-168.

Kim, J. C., Badano, J. L., Sibold, S., Esmail, M. A., Hill, J., Hoskins, B. E., Leitch, C. C., Venner, K., Ansley, S. J., Ross, A. J. et al. (2004). The Bardet-Biedl protein BBS4 targets cargo to the pericentriolar region and is required for microtubule anchoring and cell cycle progression. *Nat. Genet.* **36**, 462-470.

Klymkowsky, M. W. (1982). Vimentin and keratin intermediate filament systems in cultured PtK2 epithelial cells are interrelated. *EMBO J.* **1**, 161-165.

Lawlor, P., Marcotti, W., Rivolta, M. N., Kros, C. J. and Holley, M. C. (1999). Differentiation of mammalian vestibular hair cells from conditionally immortal, postnatal supporting cells. *J. Neurosci.* **19**, 9445-9458.

Lechler, T. and Fuchs, E. (2007). Desmoplakin: an unexpected regulator of microtubule organization in the epidermis. *J. Cell Biol.* **176**, 147-154.

Meads, T. and Schroer, T. A. (1995). Polarity and nucleation of microtubules in polarized epithelial cells. *Cell Motil. Cytoskeleton* **32**, 273-288.

Mogensen, M. M. (1999). Microtubule release and capture in epithelial cells. *Biol. Cell* **91**, 331-341.

Mogensen, M. (2004). Microtubule organising centres in polarised epithelial cells. In *Centrosomes in Development and Disease* (ed. E. A. Nigg), pp. 299-319. Weinheim: Wiley.

Mogensen, M. M., Mackie, J. B., Doxsey, S. J., Stearns, T. and Tucker, J. B. (1997). Centrosomal deployment of gamma-tubulin and pericentrin: evidence for a microtubule-nucleating domain and a minus-end docking domain in certain mouse epithelial cells. *Cell Motil. Cytoskeleton* **36**, 276-290.

Mogensen, M. M., Malik, A., Piel, M., Bouckson-Castaing, V. and Bornens, M. (2000). Microtubule minus-end anchorage at centrosomal and non-centrosomal sites: the role of ninein. *J. Cell Sci.* **113**, 3013-3023.

Mogensen, M. M., Tucker, J. B., Mackie, J. B., Prescott, A. R. and Nathke, I. S. (2002). The adenomatous polyposis coli protein unambiguously localizes to microtubule plus ends and is involved in establishing parallel arrays of microtubule bundles in highly polarized epithelial cells. *J. Cell Biol.* **157**, 1041-1048.

Moritz, M., Zheng, Y., Alberts, B. M. and Oegema, K. (1998). Recruitment of the gamma-tubulin ring complex to Drosophila salt-stripped centrosome scaffolds. *J. Cell Biol.* **142**, 775-786.

Moudjou, M., Bordes, N., Paintrand, M. and Bornens, M. (1996). gamma-Tubulin in mammalian cells: the centrosomal and the cytosolic forms. *J. Cell Sci.* **109**, 875-887.

Musch, A. (2004). Microtubule organization and function in epithelial cells. *Traffic* **5**, 1-9.

Oakley, C. E. and Oakley, B. R. (1989). Identification of gamma-tubulin, a new member of the tubulin superfamily encoded by mipA gene of Aspergillus nidulans. *Nature* **338**, 662-664.

Ohta, T., Essner, R., Ryu, J. H., Palazzo, R. E., Uetake, Y. and Kuriyama, R. (2002). Characterization of Cep135, a novel coiled-coil centrosomal protein involved in microtubule organization in mammalian cells. *J. Cell Biol.* **156**, 87-99.

Ou, Y. Y., Mack, G. J., Zhang, M. and Rattner, J. B. (2002). CEP110 and ninein are located in a specific domain of the centrosome associated with centrosome maturation. *J. Cell Sci.* **115**, 1825-1835.

Paoletti, A., Moudjou, M., Paintrand, M., Salisbury, J. L. and Bornens, M. (1996). Most of centrin in animal cells is not centrosome-associated and centrosomal centrin is confined to the distal lumen of centrioles. *J. Cell Sci.* **109**, 3089-3102.

Piel, M., Meyer, P., Khodjakov, A., Rieder, C. L. and Bornens, M. (2000). The respective contributions of the mother and daughter centrioles to centrosome activity and behavior in vertebrate cells. *J. Cell Biol.* **149**, 317-330.

Quintyne, N. J., Gill, S. R., Eckley, D. M., Crego, C. L., Compton, D. A. and Schroer, T. A. (1999). Dynactin is required for microtubule anchoring at centrosomes. *J. Cell Biol.* **147**, 321-334.

Rambhatla, L., Chiu, C. P., Glickman, R. D. and Rowe-Rendleman, C. (2002). In vitro differentiation capacity of telomerase immortalized human RPE cells. *Invest. Ophthalmol. Vis. Sci.* **43**, 1622-1630.

Reddan, J. R., Giblin, F. J., Kadry, R., Leverenz, V. R., Pena, J. T. and Dziedzic, D. C. (1999). Protection from oxidative insult in glutathione depleted lens epithelial cells. *Exp. Eye Res.* **68**, 117-227.

Schnackenberg, B. J., Khodjakov, A., Rieder, C. L. and Palazzo, R. E. (1998). The disassembly and reassembly of functional centrosomes in vitro. *Proc. Natl. Acad. Sci. USA* **95**, 9295-9300.

Stearns, T. and Kirschner, M. (1994). In vitro reconstitution of centrosome assembly and function: the central role of gamma-tubulin. *Cell* **76**, 623-637.

Stillwell, E. E., Zhou, J. and Joshi, H. C. (2004). Human ninein is a centrosomal autoantigen recognized by CREST patient sera and plays a regulatory role in microtubule nucleation. *Cell Cycle* **3**, 923-930.

Streets, A. J., Moon, D. J., Kane, M. E., Obara, T. and Ong, A. C. (2006). Identification of an N-terminal glycogen synthase kinase 3 phosphorylation site which regulates the functional localization of polycystin-2 in vivo and in vitro. *Hum. Mol. Genet.* **15**, 1465-14673.

Tucker, J. B., Paton, C. C., Richardson, G. P., Mogensen, M. M. and Russell, I. J. (1992). A cell surface-associated centrosomal layer of microtubule-organizing material in the inner pillar cell of the mouse cochlea. *J. Cell Sci.* **102**, 215-226.

Zheng, Y., Wong, M. L., Alberts, B. and Mitchison, T. (1995). Nucleation of microtubule assembly by a gamma-tubulin-containing ring complex. *Nature* **378**, 578-583.